Proc. Natl. Acad. Sci. USA
Vol. 87, pp. 6803–6807, September 1990
Biophysics

Pathway of proton transfer in bacterial reaction centers: Replacement of serine-L223 by alanine inhibits electron and proton transfers associated with reduction of quinone to dihydroquinone

(site-directed mutagenesis/bacterial photosynthesis/electron transfer/proton transfer/*Rhodobacter sphaeroides*)

M. L. PADDOCK, P. H. MCPHERSON, G. FEHER, AND M. Y. OKAMURA*

Department of Physics, B-019, University of California, San Diego, La Jolla, CA 92093

Contributed by G. Feher, June 13, 1990

ABSTRACT **The pathway of proton transfer in the reaction center (RC) from *Rhodobacter sphaeroides* was investigated by site-directed mutagenesis. Ser-L223, a putative proton donor that forms a hydrogen bond with the secondary quinone acceptor Q_B, was replaced with Ala and Thr. RCs with Ala-L223 displayed reduced electron transfer and proton uptake rates in the reaction $Q_A^-Q_B^- + 2H^+ \rightarrow Q_AQ_BH_2$. The rate constant for this reaction, $k_{AB}^{(2)}$, was found to be reduced ≈350-fold to 4.0 ± 0.2 s^{-1}. Proton uptake measurements using a pH indicator dye showed a rapid uptake of 1 H^+ per RC followed by a slower uptake of 1 H^+ per RC at a rate of 4.1 ± 0.1 s^{-1}; native RCs showed a rapid uptake of 2 H^+ per RC. Evidence is provided that these changes were not due to gross structural changes in the binding site of Q_B. RCs with Thr-L223 showed little reduction in the rates of electron and proton transfer. These results indicate that proton transfer from the hydroxyl group of Ser-L223 or Thr-L223 is required for fast electron and proton transfer associated with the formation of the dihydroquinone QH_2. In contrast, previous work showed that replacing Glu-L212, another putative proton donor to Q_B, with Gln slowed proton uptake from solution without significantly altering electron transfer. We propose a model that involves two distinct proton transfer steps. The first step occurs prior to transfer of the second electron to Q_B and involves proton transfer from Ser-L223. The second step occurs after this electron transfer through a pathway involving Glu-L212.**

The bacterial reaction center (RC) is a membrane-bound bacteriochlorophyll protein complex responsible for the light-induced electron transfer and associated proton uptake reactions in bacterial photosynthesis. The bacterial RC is composed of three subunits (L, M, and H), four bacteriochlorophylls, two bacteriopheophytins, one nonheme Fe^{2+} and two ubiquinone molecules (reviewed in refs. 1 and 2). In the RC, photochemical electron transfer reactions catalyze the sequential reduction of two quinone molecules, a tightly bound primary quinone, Q_A, and a loosely bound secondary quinone, Q_B, which serves as a mobile electron and proton carrier (reviewed in ref. 3). The reduction of Q_B to dihydroquinone Q_BH_2 involves two electron transfer reactions with rate constants $k_{AB}^{(1)}$ and $k_{AB}^{(2)}$ as shown below.

$$Q_A^-Q_B \xrightarrow{k_{AB}^{(1)}} Q_AQ_B^- \quad [1]$$

$$Q_A^-Q_B^- + 2H^+ \xrightarrow{k_{AB}^{(2)}} Q_AQ_BH_2 \quad [2]$$

In reaction 2 the second electron transfer is coupled to the uptake of two protons from solution. On the basis of investigations of the kinetics of electron transfer and proton uptake from solution, a mechanism for the sequence of these electron and proton transfer steps has been proposed (4); however, the molecular pathways for these proton transfer steps have not been established. After reduction to Q_BH_2, the dihydroquinone dissociates from the RC (5). In photosynthetic membranes reoxidation of QH_2 releases protons on the periplasmic side of the membrane, resulting in the formation of a proton gradient. This proton gradient gives rise to an electrochemical gradient that drives ATP synthesis (6, 7).

The Q_B binding site is in the interior of the protein and is formed mainly by amino acid residues of the L subunit (8). The observation of rapid proton uptake accompanying the reduction of Q_B, buried in the interior of the protein, out of contact with the aqueous solution, led to the hypothesis that a proton transfer pathway via protonatable residues exists in the protein, allowing access of protons from solution to Q_B. The structure of the RC from *Rhodobacter* (*Rb.*) *sphaeroides* suggests two possible pathways for this proton conduction (8). One leads from the cytoplasmic side of the protein through part of the H, M, and L subunits through Glu-L212 to the quinone carbonyl group close to His-L190. A second pathway leads from the cytoplasmic side of the RC near the proposed membrane surface through Ser-L223 to the other quinone carbonyl group.

One proton pathway was investigated by site-directed mutagenesis of a putative proton donor residue, Glu-L212, in the vicinity of Q_B (9). The change of Glu-L212 to Gln resulted in a significantly slower proton uptake (10) with relatively little change in the measured electron transfer rates of the first and second electron ($k_{AB}^{(1)}$ or $k_{AB}^{(2)}$) (9). Normal proton uptake rates were observed in RCs with Asp replacing Glu-L212 (11). These results show that Glu-L212 plays a role in proton uptake and support the concept of a proton transfer chain to the Q_B pocket.

In this study we examined the second proton pathway, involving Ser-L223. The hydroxyl group of the Ser-L223 forms a hydrogen bond to one carbonyl oxygen of the quinone (8), providing a possible path for proton transfer. Mutant RCs were isolated in which Ser-L223 was replaced with either Ala or Thr, resulting in SA(L223) and ST(L223) mutant RCs, respectively. The following electron and proton transfer properties of these mutant RCs were studied: (*i*) the rates of electron transfer to Q_B and Q_B^-, (*ii*) the cycling rate of electrons from cytochrome *c* (cyt *c*) to exogenous quinone through the RC, and (*iii*) the stoichiometry and kinetics of proton uptake by the RC from solution. A model to explain these observations is discussed.

MATERIALS AND METHODS

Site-Directed Mutagenesis. The mutants were constructed as described in ref. 9 with a few modifications noted below.

The publication costs of this article were defrayed in part by page charge payment. This article must therefore be hereby marked "*advertisement*" in accordance with 18 U.S.C. §1734 solely to indicate this fact.

Abbreviations: D, primary donor; Q_A, primary quinone acceptor; Q_B, secondary quinone acceptor; QH_2, dihydroquinone; UQ_{10}, ubiquinone-50; RC, reaction center; cyt *c*, horse heart cytochrome *c*; DAD, 2,3,5,6-tetramethyl-1,4-phenylenediamine (diaminodurene).

*To whom reprint requests should be addressed.

The site-directed mutagenesis was performed by using the Amersham oligonucleotide-directed mutagenesis kit. A mixed oligonucleotide was synthesized to direct the mutagenesis: 5′-CGGCTAC(G/A)CCATCGGGACGCT-3′, where the GCC codon for Ala or the ACC codon for Thr replaced the native TCG codon for Ser-L223. The mutations were incorporated into an M13 vehicle containing the *Pvu* II–*Sal* I fragment [490 base pairs (bp)], replacing the pUC119 vehicle used in ref. 9. The complemented deletion strains were grown semiaerobically to induce RC production without applying selection for photosynthetic growth. The analogous mutation has been reported in *Rhodobacter capsulatus* (12).

RC Preparation. RCs were isolated in *N,N*-dimethyldodecylamine *N*-oxide (LDAO; Fluka Chemie) as described (13); they contained approximately one quinone per RC as determined by standard methods (14) with an absorbance ratio of $A_{280}/A_{802} < 1.3$. RC concentrations were determined from the amount of cyt *c* oxidized (measured at 550 nm) after one flash, using $\epsilon_{550} = 21.1\ mM^{-1}\cdot cm^{-1}$ (15). Reconstitution of Q_B into the mutant RCs was accomplished as follows: a 5- to 10-fold excess of ubiquinone-50 (UQ_{10}) was added to the RC solutions ($A_{802}^{1\ cm} \approx 2$), which were then dialyzed for 2 days against 2 mM Hepes, pH 7.5/0.04% dodecyl β-D-maltoside (Calbiochem)/8 mM KCl. Native RCs were reconstituted with Q_B by the same procedure except that 2 UQ_{10} molecules per RC were added. The reconstituted RCs were concentrated to $A_{802}^{1\ cm} \geq 50$.

Electron Transfer Rate Measurements. The kinetics of absorbance changes were recorded on a modified Cary 14 spectrophotometer (Varian) as described in ref. 14. All measurements were performed at an RC concentration of 1–3 μM in HMK buffer (10 mM Hepes, pH 7.5/0.04% dodecyl β-D-maltoside/50 mM KCl) at 23°C. The rate constant $k_{AB}^{(1)}$ (Eq. 1) was obtained from the absorbance changes at 745 nm (14). The rate constant $k_{AB}^{(2)}$ (Eq. 2) was obtained from the decay of the semiquinone absorbance at 450 nm (16), using 500 μM 2,3,5,6-tetramethyl-1,4-phenylenediamine (DAD) to reduce the donor (D) after a flash. The charge recombination rates from $D^+Q_A^-$ to DQ_A (k_{AD}) were determined from the rate of recovery of the oxidized donor (D^+) monitored at 865 nm in RCs containing only Q_A. The charge recombination rates from $D^+Q_AQ_B^-$ to DQ_AQ_B (k_{BD}) were determined from the kinetics of the slow phase of the donor recovery (≈90% of the amplitude) in RC samples in the presence of excess UQ_{10}; the remaining ≈10% was attributed to the fraction of RCs without a bound Q_B.

Cytochrome turnover rates were measured by monitoring the oxidation of cyt *c* (type 6, Sigma) at 550 nm (see, e.g., ref. 13) in the presence of excess UQ_{10} under continuous illumination ($I = 1\ W\cdot cm^{-2}$, white light). RCs were illuminated perpendicular to the monitoring beam of a Cary 14 spectrophotometer with a short saturating pulse ($\Delta t_{1/e} = 1.5$ ms, pulse energy = 80 mJ) from a Norman P2000D flash lamp followed by continuous illumination from a 500-W projector through 1 inch (2.54 cm) of water and a Corning 2-64 filter. (Conditions: 0.7–1.0 μM RCs with excess UQ_{10} in HMK buffer with 25–50 μM cyt *c*.) The rate of cyt *c* turnover was determined from the absorbance change at 550 nm normalized to the absorbance change at 550 nm after a single flash (representing one cyt *c* oxidized per RC).

Proton Uptake Measurements. Proton uptake was determined from the absorbance change at 557 nm of the pH indicator dye phenol red (Sigma; $pK_a \approx 7.7$), following a saturating light pulse (of sufficient duration to reduce all of the UQ_{10}) from a Norman P2000D flash lamp ($\Delta t_{1/e} = 1.5$ ms, pulse energy = 80 mJ). Corrections (5–10%) due to absorbance changes of RCs and cyt *c* were determined from the absorbance changes of a strongly buffered sample (20 mM Hepes, pH 7.5). The proton uptake was calibrated by adding known amounts of HCl. Carbon dioxide was excluded from the cuvette by a flow of wet argon. The water (double-distilled in quartz) for the proton uptake solutions was degassed by boiling under argon. Native RCs contained an average of 1.93 quinones as determined by the amount of cyt *c* oxidized after a saturating light pulse from the flash lamp. SA(L223) RCs contained a 5- to 10-fold excess of UQ_{10} per RC to maximize the occupancy of the Q_B site. (Conditions: 1.5 μM RCs, 25 μM cyt *c*, 50 μM phenol red, 50 mM KCl, 0.04% dodecyl β-D-maltoside, pH 7.5, 23°C.)

EPR Spectroscopy. Electron paramagnetic resonance (EPR) measurements were made as described earlier (17). Samples containing $DQ_A\bar{Q}_B$ were obtained by rapid freezing after a single laser flash in the presence of cyt *c* and excess UQ_{10}. (Conditions: 70 μM RCs in pH 7.5 HMK, 1 mM cyt *c*, 2.1°C, microwave frequency $\nu_e = 8.8$ GHz.)

RESULTS AND ANALYSIS

Cytochrome Turnover. The overall rate of the photocycle (Fig. 1) was measured by monitoring the oxidation of cyt *c* in the presence of excess cyt *c* and quinone. Reductions in the rates of the electron or proton transfer reactions will reduce the cyt *c* turnover rate if they become the rate-limiting step.

The cytochrome turnover rates for native and SA(L223) RCs are shown in Fig. 2. The native RCs showed a fast turnover rate of ≥500 (cyt/RC)·s^{-1} (Table 1). The SA(L223) RCs showed a rapid oxidation ($k > 500\ s^{-1}$) of 2.0 ± 0.1 cyt/RC, followed by a slower turnover at a rate of 8.0 ± 0.4 (cyt/RC)·s^{-1}. Since two cyt *c* molecules are oxidized per cycle (Fig. 1), this corresponds to a cycling rate of 4.0 ± 0.2 s^{-1}. The ST(L223) RCs had a rate of cytochrome turnover of ≈200 (cyt/RC)·s^{-1}, which is similar to the rate in native RCs.

The fast oxidation of two cyt *c* molecules by SA(L223) RCs indicates that $Q_A^-Q_B^-$ is formed quickly (Fig. 1). The slow turnover rate suggests, however, that the subsequent step ($k_{AB}^{(2)}$) is rate limiting. A molecular picture of this electron (and accompanying proton) transfer process will be discussed later.

Electron Transfer Rates. The electron transfer rates for the individual steps in the photocycle were measured by transient optical absorption techniques. In the SA(L223) RCs, the rate constant for the transfer of the first electron, $k_{AB}^{(1)}$, was determined from the absorbance change of bacteriopheophytin at 745 nm upon electron transfer. It was found to be 15,000 s^{-1}, greater than the value of 6,000 s^{-1} observed in native RCs (Table 1). The measured rate constant for the transfer of the second electron to Q_B, $k_{AB}^{(2)}$, was obtained from the absorbance decay of the semiquinone monitored at 450 nm

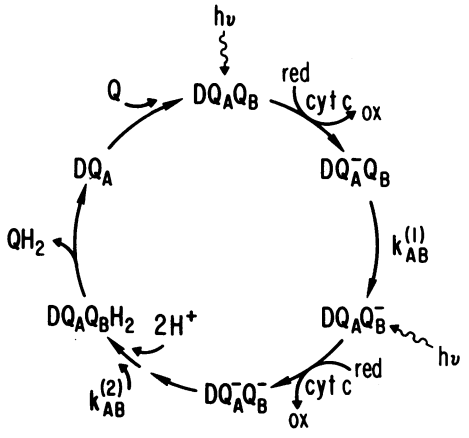

FIG. 1. Model for cytochrome photooxidation. The cycle consists of electron transfer, proton uptake, and quinone exchange. The cycling rate for native RCs is ≥ 250 s^{-1} (Fig. 2). red, reduced; ox, oxidized.

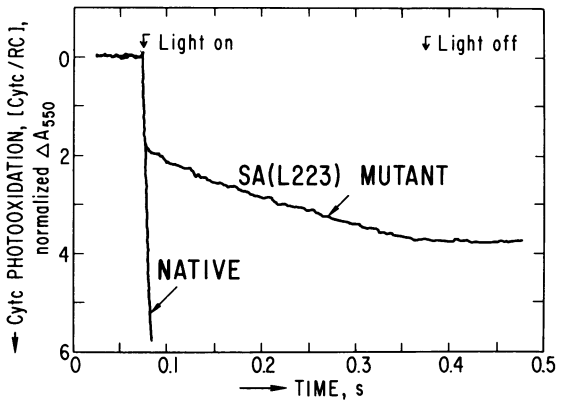

FIG. 2. Cytochrome photooxidation in native and SA(L223) mutant RCs. In Figs. 2–5, arrows on axes indicate direction of increase. Photooxidation of cyt *c* was monitored at 550 nm in the presence of exogenous quinone under continuous illumination. (Conditions: 0.7 μM RCs, 50 μM cyt *c*, 10 mM Hepes at pH 7.5, 0.04% dodecyl β-D-maltoside, 50 mM KCl, I = 1 W·cm^{-2}, 23°C.) The cyt *c* turnover rate for native RCs was 500 (cyt/RC)·s^{-1}. The SA(L223) mutant RCs show a fast oxidation of two cyt *c* followed by a slow turnover at a rate of 8 (cyt/RC)·s^{-1}, indicating that $DQ_A^-Q_B^-$ is formed quickly and that $k_{AB}^{(2)}$ is reduced in the mutant.

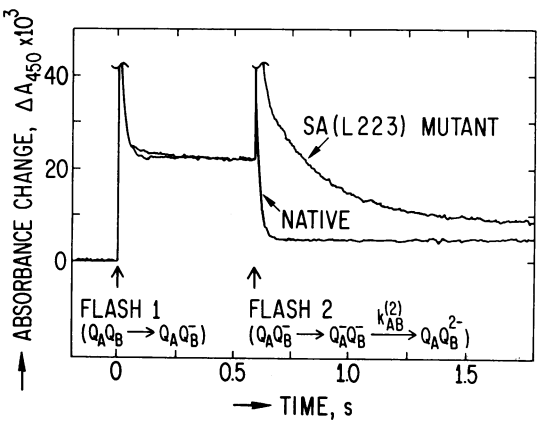

FIG. 3. Transfer kinetics of the second electron to Q_B. The absorbance of semiquinone was monitored at 450 nm as a function of time. The absorbance increased after the first flash due to the formation of $Q_AQ_B^-$. A transient absorbance increase due to the formation of the $Q_A^-Q_B^-$ state was seen after the second flash. In native RCs this absorbance decayed rapidly due to the formation of the doubly reduced Q_B state with a rate constant of 1500 s^{-1} (not observable under these conditions). In the SA(L223) mutant the semiquinone absorbance decayed slowly with a rate constant of 4 s^{-1} due to the slow formation of $Q_AQ_BH_2$. A spike (cut off in the figure) was observed after each flash due to the absorption at 450 nm by D^+, which was reduced in ≈50 ms by DAD. (Conditions: ≈3 μM RCs, 500 μM DAD, 10 mM Hepes at pH 7.5, 0.04% dodecyl β-D-maltoside, 50 mM KCl, 23°C.) The traces were adjusted to have the same absorbance after the first flash. The residual absorbance change seen at long times after double reduction of Q_B was due to the absorbance of the residual semiquinone Q_A^- caused by (*i*) RCs without a bound Q_B prior to the first flash and (*ii*) the equilibrium fraction of RCs in the $DQ_A^-Q_B$ state after the first flash.

after the second flash (Fig. 3). In native RCs the absorbance decayed rapidly with a rate constant $k_{AB}^{(2)}$ = 1500 s^{-1}. However, in the SA(L223) RCs, $k_{AB}^{(2)}$ is only 4.0 ± 0.2 s^{-1}, which is a factor of 350 smaller than that observed in native RCs (Table 1). This rate is equal to the cycling rate determined from the cyt *c* turnover measurements, consistent with $k_{AB}^{(2)}$ being the rate-limiting step in the photocycle.

The recombination rate, k_{AD} ($D^+Q_A^- \rightarrow DQ_A$), in RCs containing only Q_A was found to be the same in native and SA(L223) RCs ($k_{AD} \approx 9$ s^{-1}). The recombination rate, k_{BD} ($D^+Q_AQ_B^- \rightarrow DQ_AQ_B$), obtained from the kinetics of the slow phase in the presence of excess UQ_{10} was found to be slightly slower in the SA(L223) RCs (k_{BD} = 0.62 s^{-1}) than in native RCs (k_{BD} = 0.70 s^{-1}). The small value of k_{BD} indicates that $Q_AQ_B^-$ is stabilized with respect to $Q_A^-Q_B$ (14).

Proton Uptake. The proton uptake by native and SA(L223) RCs was determined by measuring the absorbance changes of the pH indicator dye phenol red after illumination with a saturating light pulse in the presence of cyt *c* (Fig. 4).

Illumination of *native* RCs caused the rapid (k > 500 s^{-1}) formation of $DQ_A^-Q_B^{2-}$; electron turnover to exogenous quinone was prevented by decreasing the quinone concentration to less than 2 per RC (1.93 UQ_{10} per RC). The observed proton uptake (Fig. 4 *Upper*) was rapid (k > 500 s^{-1}) and had a value of 2.0 H^+ per RC. This value was corrected for the proton release from the oxidized cyt *c* [≈0.1 H^+ (18)] and for the fraction of RCs that lacked a bound Q_B (≈0.15 H^+). The corrected value of 2.3 H^+ per $DQ_A^-Q_B^{2-}$ is consistent with the uptake of two protons by Q_B^{2-} to form Q_BH_2 and an additional uptake of 0.3 proton due to the pK_a shifts of amino acid residues that interact with Q_A^- (18).

Illumination of the *SA(L223)* RCs (Fig. 4 *Lower*) caused the rapid (k > 500 s^{-1}) formation of the state $DQ_A^-Q_B^-$, which was accompanied by the uptake of 1.0 H^+. These protons were assumed to be taken up by amino acid residues that interact with Q_A^- and Q_B^-. Previous measurements (18) indicated that pK_a shifts associated with the formation of either DQ_A^- or $DQ_AQ_B^-$ cause an uptake of ≈0.4 H^+ at pH 7.5. A slower (k = 4.1 ± 0.1 s^{-1}) uptake of an additional 1.0 H^+ was observed concomitant with the formation of $DQ_AQ_B^{2-}$ (Fig. 3). No correction for the observed proton uptake was necessary since the proton release by the oxidized cyt *c* (≈0.06 H^+) and the proton uptake (≈0.08 H^+) due to the reduction of a small fraction of exogenous quinone approximately cancelled. The

Table 1. Electron transfer of native and Ser-L223 mutant RCs (pH 7.5)

Reaction	Rate constant	Assay	Rate, s^{-1} Native*	SA(L223)	ST(L223)†
cyt *c* turnover (cyt/RC)	k	1	≥500	8	≈200
$D^+Q_A^- \rightarrow DQ_A$	k_{AD}	2	9.0	9.1	8.7
$DQ_A^-Q_B \rightarrow DQ_AQ_B^-$	$k_{AB}^{(1)}$	3	6000	15,000	—
$D^+Q_AQ_B^- \rightarrow DQ_AQ_B$	k_{BD}	4	0.70	0.62	—
$DQ_A^-Q_B^- \rightarrow DQ_AQ_B^{2-}$	$k_{AB}^{(2)}$	5	1500	4	—

RC concentrations were 1–3 μM, except in assay 1. Assay 1: cyt *c* oxidation monitored at 550 nm (13) (0.3–1.0 μM RCs with excess UQ_{10} and 25–50 μM cyt *c* in HMK buffer). Assay 2: donor recovery monitored at 865 nm (14) (RCs with only Q_A). Assay 3: bacteriopheophytin bandshift monitored at 747 nm (14). Assay 4: donor recovery monitored at 865 nm (14). Assay 5: semiquinone signal monitored at 450 nm (16) (RCs with 500 μM DAD in HMK buffer). There was a variation of ≈5% in the rates, depending on the particular RC preparation and age of the sample.

*Native represents R26 or 2.4.1 RCs; the two strains gave the same results.

†The rates involving Q_B were not determined because of the low (5–10%) occupancy of the Q_B site.

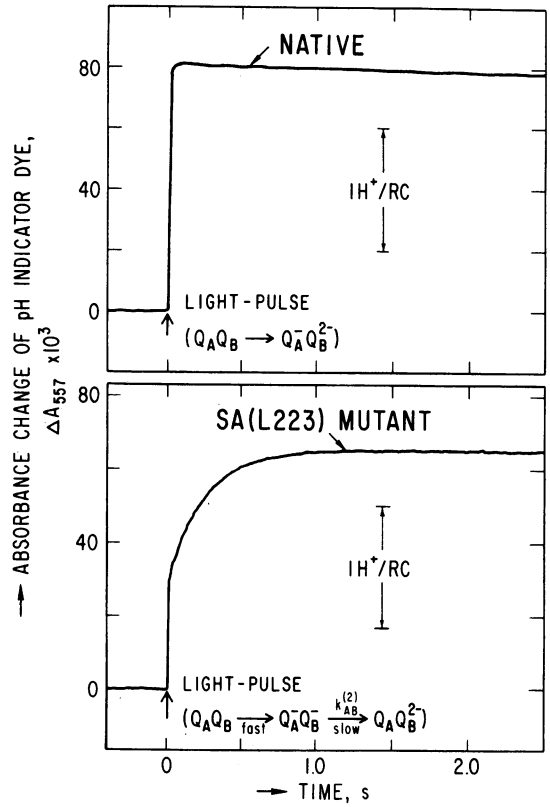

FIG. 4. Proton uptake by native (*Upper*) and the SA(L223) mutant (*Lower*) RCs in the presence of exogenous cyt *c* after a saturating light pulse ($\Delta t_{1/e}$ = 1.5 ms, pulse energy = 80 mJ). A small background signal (≈5% of the total amplitude) due to absorbance changes of the RCs and cyt *c* has been subtracted. The proton uptake was calibrated by adding a known amount of HCl. The native RCs, containing 1.93 quinone molecules per RC, take up 2.0 H^+ per RC quickly ($k > 500\ s^{-1}$), indicating that Q_BH_2 is formed in <2 ms. The SA(L223) mutant RCs with excess UQ_{10} present (to maximize the amount of bound Q_B) take up 1.0 H^+ per RC quickly and then take up an additional 1.0 H^+ per RC with a rate constant of 4 s^{-1}. The slow proton uptake is concomitant with transfer of the second electron. (Conditions: 1.5 μM RCs, 25 μM cyt *c*, 50 μM phenol red, 50 mM KCl, 0.04% dodecyl β-D-maltoside, pH 7.5, 23°C.)

uptake of a total of 2.0 H^+ per $DQ_AQ_B^{2-}$ is consistent with the formation of QH_2.

EPR Spectroscopy. The EPR spectrum of Q_B^- was measured in SA(L223) and native RCs to test the possibility that the reduced rate of electron transfer ($k_{AB}^{(2)}$) was due to a change in the structure of the Q_B^- site. The spectrum of Q_B^- in SA(L223) RCs was very similar to the spectrum in native RCs (Fig. 5). The spectrum of Q_A^- in the SA(L223) RCs was also essentially identical to that in native RCs (data not shown) and was distinct from the spectrum of Q_B^-. Since the EPR spectrum is sensitive to changes in the structure of the binding site, these spectra indicate that the structure of the Q_B^- site, in particular the distance between Q_B^- and Fe^{2+}, is not significantly altered in the mutant.

DISCUSSION

We have constructed and characterized RCs from *Rb. sphaeroides* in which Ser-L223 was changed to Ala or Thr. The replacement of Ser-L223 by Ala [SA(L223) mutation] resulted in a large (≈350-fold) decrease in the measured rate constant $k_{AB}^{(2)}$ for the transfer of the second electron to Q_B and a reduced rate of proton uptake associated with this process. The replacement of Ser-L223 by Thr had little effect on the electron and proton transfer rates. We propose that these changes result from the loss of proton transfer to reduced Q_B

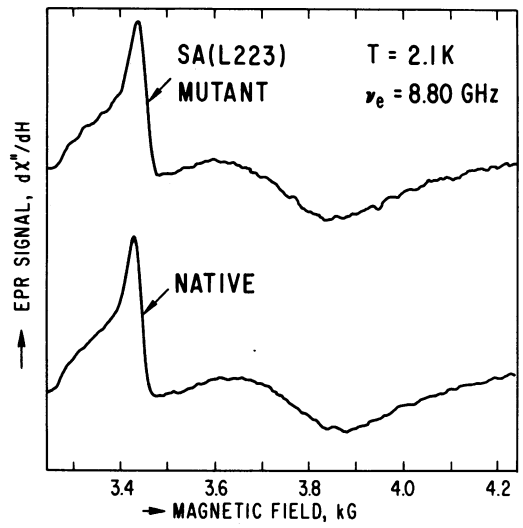

FIG. 5. EPR spectra of $Q_AFe^{2+}Q_B^-$ in the SA(L223) mutant and native RCs. The similarity of the spectra indicates that the structure of the Q_B^- site is not significantly altered in the mutant. (Conditions: 70 μM RCs in HMK at pH 7.5, 1 mM cyt *c*, 2.1 K, ν_e = 8.8 GHz.)

by the hydrogen-bonded hydroxyl group of Ser-L223 and are not due to possible conformational charges brought about by the mutation. Evidence for this is provided by the results from the ST(L223) RCs, in which the proton and electron transfer rates were not appreciably changed. If the observed changes in the SA(L223) RCs were due to conformational changes other than the removal of the hydroxyl group, similar changes would be expected in the ST(L223) RCs. Further evidence is provided by the observation that properties of Q_B in the SA(L223) RCs that are not associated with proton uptake remained essentially unaltered. These include the electron transfer rate for the one-electron reduction ($k_{AB}^{(1)}$) of Q_B, the Q_B binding strength, and the recombination rate constant k_{BD}. Furthermore, the EPR spectrum indicates that the interaction (i.e., distance) between Q_B^- and Fe^{2+} remained unchanged.

General Mechanism of Protonation. Protonation lowers the electrostatic energy of reduced quinone. Since the pK_a values for QH_2 and QH are 12–13 and 5–6, respectively (19), only Q_B^{2-} is appreciably protonated at physiological pH. This accounts for the uptake of two protons when the second electron is transferred to Q_B^-. However transient protonation of Q_B^- may affect the rate of electron transfer by lowering the energy barrier to reach the doubly reduced product state.

Proton transfer to the reduced Q_B can be divided into two types of processes. The first process involves the *internal* proton transfer within the hydrogen bond(s) to the quinone carbonyl groups made by Ser-L223 and possibly His-L190; they represent the *primary* proton transfer(s) to the quinone. This proton transfer(s) may be strongly coupled to electron transfer. Fluctuations in the proton position within the hydrogen bond(s) may be responsible for the fluctuations in energy required to achieve electron transfer. The second process involves the transfer of *external* protons through a series of secondary proton donors of the protein to reprotonate the primary proton donors (e.g., see refs. 20–22). It may not be required for fast electron transfer but is required for the completion of the photocycle (Fig. 1). The observation that replacement of Glu-L212 with Gln reduced the rate of proton transfer (10) but did not substantially change the rate of electron transfer (9) strongly suggests that Glu-L212 is a secondary proton donor. The observation that the replacement of Ser-L223 with Ala resulted in a large reduction in the proton (Fig. 4) and electron (Fig. 3) transfer rates and its

proximity to Q_B strongly suggest that Ser-L223 is a primary proton donor.

It is surprising that the loss of the hydrogen bond from the hydroxyl group in the SA(L223) RCs does not destabilize Q_B^- (as indicated by the unchanged k_{BD}). A possible explanation is that alternative hydrogen bonds to Q_B^- may be formed by peptide NH groups as seen in *Rhodopseudomonas viridis* (23). However a peptide hydrogen bond lacks the ability to simultaneously donate and accept a proton and thus is not capable of serving in a hydrogen-bonded chain (20).

Molecular Model of Electron and Proton Transfers. A mechanism for the electron transfer leading to the formation of QH_2 is shown in Fig. 6. It involves three steps (Fig. 6*a*): (*i*) protonation of Q_B^-, (*ii*) transfer of the second electron, forming Q_B^-H, and (*iii*) proton uptake to form Q_BH_2. Two models in which electron transfer either precedes or follows (our model) proton uptake have been proposed by Maròti and Wraight (4).

The molecular details of this model, consistent with our results on the mutant RCs, are shown in Fig. 6*b*. The first proton, $H^+(1)$, *preceding* the transfer of the second electron, is transported along a pathway involving Ser-L223. The uptake of the second proton, $H^+(2)$, *following* the second electron transfer, is transported along a pathway involving Glu-L212. This mechanism is consistent with the assignment of Ser-L223 as a primary proton donor and Glu-L212 as a secondary proton donor. This model also explains the pH dependence of $k_{AB}^{(2)}$ (4, 16); i.e., at lower pH the proton uptake by Q_B^- is enhanced [see $H^+(1)$ in Fig. 6].

In conclusion, the two-pathway model requiring proton transfer from Ser-L223 prior to electron transfer and fast proton transfer from Glu-L212 after electron transfer is consistent with all kinetic measurements for the native and mutant RCs. Several questions remain to be answered: (*i*) Is internal proton transfer from other primary proton donors (e.g., His-L190) obligatory for the transfer of the second electron? and (*ii*) What other groups are involved in the proton transfer pathways? Further experiments on modified RCs should answer these questions.

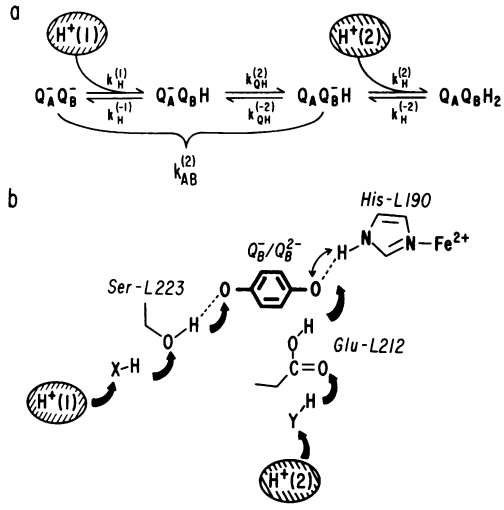

FIG. 6. Schematic representation of the dihydroquinone Q_BH_2 formation. (*a*) The temporal order of the various proton and electron transfer reactions that lead to the formation of QH_2. H^+ represent protons from solution that transfer into the pocket via different proton transfer chains (see below). (*b*) Proposed structural details of proton and electron transfer steps involved in reducing Q_B^- to Q_BH_2. The first proton, $H^+(1)$, is transferred to Q_B^- via a pathway involving Ser-L223; X-H represents another protonatable residue in a chain connecting Ser-L223 to the solvent (possibly Arg-L217 or Asp-L213). The second proton, $H^+(2)$, is transferred via a pathway involving Glu-L212; Y-H represents the next group in the chain connecting Glu-L212 with the solvent (possibly a water molecule). The role of the proton on His-L190 (see double-headed arrow) has so far not been elucidated. This scheme is based on the structure described in ref. 8.

Note Added in Proof. We have recently replaced Asp-L213 with Asn or Leu. In these mutants the transfer rate of the second electron was reduced ≈500-fold; the transfer rate of the first electron was reduced only ≈4-fold. These results suggest that Asp-L213 is involved in the proton transfer chain for $H^+(1)$ (most likely X-H in Fig. 6*b*) and that Ser-L223 cannot transfer its proton to Q_B^- without simultaneously receiving a proton.

We thank Ed Abresch for purification of the RCs and R. Isaacson, A. Juth, and R. Dicker for technical assistance. This work was supported by grants from the National Institutes of Health (1 R01GM41637) and the National Science Foundation (DMB89-06055 and DMB85-18922).

1. Feher, G., Allen, J. P., Okamura, M. Y. & Rees, D. C. (1989) *Nature (London)* **339,** 111–116.
2. Breton, J. & Vermeglio, A., eds. (1988) *The Photosynthetic Bacterial Reaction Center: Structure and Dynamics* (Plenum, New York).
3. Crofts, A. R. & Wraight, C. A. (1983) *Biochim. Biophys. Acta* **726,** pp. 149–185.
4. Maròti, P. & Wraight, C. A. (1990) in *Current Research in Photosynthesis,* ed. Baltscheffsky, M. (Kluwer, Boston), Vol. 1, pp. 1.165–1.168.
5. McPherson, P. H., Okamura, M. Y. & Feher, G. (1990) *Biochim. Biophys. Acta* **1016,** 289–292.
6. Dutton, P. L. (1986) in *Photosynthesis III: Photosynthetic Membranes and Light Harvesting Systems, Encyclopedia of Plant Physiology,* eds. Staehlin, L. A. & Arntzen, C. J. (Springer, New York), Vol. 19, pp. 197–237.
7. Ort, D. R. (1986) in *Photosynthesis III: Photosynthetic Membranes and Light Harvesting Systems, Encyclopedia of Plant Physiology,* eds. Staehlin, L. A. & Arntzen, C. J. (Springer, New York), Vol. 19, pp. 143–196.
8. Allen, J. P., Feher, G., Yeates, T. O., Komiya, H. & Rees, D. C. (1988) *Proc. Natl. Acad. Sci. USA* **85,** 8487–8491.
9. Paddock, M. L., Rongey, S. H., Feher, G. & Okamura, M. Y. (1989) *Proc. Natl. Acad. Sci. USA* **86,** 6602–6606.
10. McPherson, P. H., Schönfeld, M., Paddock, M. L., Feher, G. & Okamura, M. Y. (1990) *Biophys. J.* **57,** 404 (abstr.).
11. Paddock, M. L., Feher, G. & Okamura, M. Y. (1990) *Biophys. J.* **57,** 569 (abstr.).
12. Bylina, E. J., Jovine, R. V. M. & Youvan, D. C. (1989) *Bio/Technology* **7,** 69–74.
13. Paddock, M. L., Rongey, S. H., Abresch, E. C., Feher, G. & Okamura, M. Y. (1988) *Photosynth. Res.* **17,** 75–96.
14. Kleinfeld, D., Okamura, M. Y. & Feher, G. (1984) *Biochim. Biophys. Acta* **766,** 126–140.
15. Van Gelder, B. F. & Slater, E. C. (1962) *Biochim. Biophys. Acta* **58,** 593–595.
16. Kleinfeld, D., Okamura, M. Y. & Feher, G. (1985) *Biochim. Biophys. Acta* **809,** 291–310.
17. Butler, W. F., Calvo, R., Fredkin, D. R., Isaacson, R. A., Okamura, M. Y. & Feher, G. (1984) *Biophys. J.* **45,** 947–973.
18. McPherson, P. H., Okamura, M. Y. & Feher, G. (1988) *Biochim. Biophys. Acta* **934,** 348–368.
19. Morrison, L. E., Schelhorn, J. E., Cotton, T. M., Bering, C. L. & Loach, P. A. (1982) in *Function of Quinones in Energy Conserving Systems,* ed. Trumpower, B. L. (Academic, New York), pp. 35–58.
20. Nagle, J. & Tristram-Nagle, S. (1983) *J. Membr. Biol.* **74,** 1–14.
21. Schulten, Z. & Schulten, K. (1986) *Methods Enzymol.* **127,** 419–438.
22. Warshel, A. (1986) *Methods Enzymol.* **127,** 578–587.
23. Sinning, I., Koepke, J., Schiller, B. & Michel, H. (1990) *Z. Naturforsch.* **45,** pp. 455–458.